

## A Numerical Simulation of MHD Flow and Radiation Heat Transfer of Nanofluids Through a Porous Medium with Variable Surface Heat Flux and Chemical Reaction

**E. Hosseini**  
Yazd University

**Gh. Barid Loghmani\***  
Yazd University

**M. Heydari**  
Yazd University

**M. M. Rashidi**  
University of Birmingham

**Abstract.** In this paper, the problem of MHD flow and radiation heat transfer of nanofluids against a flat plate in porous medium with the effects of variable surface heat flux and first-order chemical reaction is investigated numerically. Three different types of nanoparticles, namely Cu,  $\text{Al}_2\text{O}_3$  and Ag are considered by using water as a base fluid with Prandtl number  $Pr = 6.2$ . The governing partial differential equations can be written as a system of nonlinear ordinary differential equations over a semi-infinite interval using a similarity transformation. A new effective collocation method is proposed based on exponential Bernstein functions to simulate the solution of the resulting differential systems. The advantage of this method is that it does not require truncating or transforming the semi-infinite domain of the problem to a finite domain. In addition, this method reduces the solution of the problem

---

Received: November 2017; Accepted: May 2018

\*Corresponding author

to the solution of a system of algebraic equations. Graphical and tabular results are presented to investigate the influence of the solid volume fraction, types of nanoparticles, radiation and suction/blowing, magnetic field, permeability, Schmidt number and chemical reaction, on velocity, temperature and concentration profiles. The obtained results of the current study are in excellent agreement with previous works.

**AMS Subject Classification:** 65N35; 35G60; 41A04; 76S05

**Keywords and Phrases:** Boundary layer flow, MHD flow, nanofluids, exponential bernstein functions, collocation method

## 1. Introduction

In recent years, the boundary layer flow and heat transfer of nanofluids have received considerable attention due to its wide applications in industry, technological and natural processes. The researchers of fluid dynamics are showing that the commonly using metals exhibit high thermal conductivity compared with the fluids. Thus, for increasing the heat transfer capability of the fluids require to mix both the fluid and metals. Initially, the concept of ‘nanofluids’ was considered by Choi et al. [16] for suspension of liquids containing ultra-fine particles (diameter less than 50 nm). The base fluids used are usually water, oil, ethylene glycol or toluene and nanoparticles include metals such as copper, aluminum, iron, gold, silver and titanium or their oxides. The effect on the thermal conductivity of nanofluids is different for the base fluid material, particle size, particle material, temperature, particle volume concentration,  $PH$  value of the base fluid and the shape, size and volume fraction of the nanoparticles. Typical thermal conductivity enhancements are in the range 15% – 40% with low concentration (1 – 5 by volume) of the solid nanoparticles in the mixture. Therefore, the nanofluids are suitable alternative to many common fluids for advanced thermal applications and play a major role in heat transfer, fuel cells, chiller, pharmaceutical processes, hybrid-powered engines, space technology, boiler flue gas temperature reduction including microelectronics, domestic refrigerator, nuclear reactor coolant and in grinding. Referring to the potential of nanofluids in advanced nuclear systems, Masuda et al. [46] illustrated that nanofluids have an abnormal enhancement in thermal

conductivity. Buongiorno [13] has studied the convective transport phenomena in nanofluid. He considered in turn seven slip mechanisms and showed that Brownian diffusion and thermophoresis diffusion models are the two most important nanoparticle/base-fluid slip mechanisms among these mechanisms. Some study on the nanofluids with considering the Brownian diffusion and thermophoresis diffusion done by Makinde [39], Ibrahim et al. [29] and Garoosi et al. [21]. Also, on these two slip mechanisms, Makinde et al. [36, 37] presented the boundary layer flow of nanofluids over a moving flat plate and Kuznetsov et al. [35] introduced natural convective boundary layer flow of a nanofluid over a vertical plate.

Stagnation flow, analysis the fluid movement near the stagnation-point, occurs on all solid particles moving in a fluid. The highest heat transfer, highest pressure and highest rate of mass decomposition happening in the stagnation-point. Stagnation flow of viscous fluids arise in many applications like the flows over the tips of rockets, submarines, aircrafts and oil ships. At first, Hiemenz [25] investigated the stagnation flow problem using linear group of transformations. Wang [53] analyzed the stagnation flow of two fluids with different densities. Chiam [15] presented the steady stagnation-point flow over an elastic surface considering the equal values of the stretching and straining velocity. Recently, Alsaedi et al. [1] investigated the effects of heat generation/absorption on stagnation-point flow of nanofluid over a surface with convective boundary conditions. Bachok et al. [4] proposed boundary layer stagnation-point flow and heat transfer over an exponentially stretching/shrinking sheet in a nanofluid. Anwar et al. [3] analyzed MHD and radiation effects on stagnation point flow of nanofluid towards a nonlinear stretching sheet. The steady boundary-layer flow near the stagnation point on an impermeable vertical surface with slip that is embedded in a fluid-saturated porous medium was done by Harris et al. [22]. Pal et al. [50] employed numerical method to study the influence of thermal radiation on mixed convection heat and mass transfer stagnation-point flow in nanofluids over stretching/shrinking sheet in a porous medium with chemical reaction.

Bernstein polynomials have important applications in computer graphics and have been applied for approximations of functions in many areas of mathematics and other fields such as smoothing in statistics and constructing Bézier curves [19, 20, 33]. These polynomials were first used by Sergei Natanovich Bernstein in a constructive proof for the Stone-Weierstrass approximation theorem. Bernstein polynomials have been applied to solve various kinds of ordinary and partial differential equations, integral equations and integro-differential equations defined in engineering and science [6, 24]. Recently, Heydari et. al [23] applied the Gram-Schmidt orthogonalization process to find orthogonal Bernstein polynomials for the solution of heat transfer of a micropolar fluid through a porous medium with radiation.

The aim of the present work is study MHD flow and radiative heat transfer of a nanofluid against a flat plate in porous media with variable wall temperature and a first-order chemical reaction. The governing nonlinear ordinary differential equations are solved numerically by using a collocation method based on exponential Bernstein functions for three types of nanoparticles. Assuming small Reynolds number, the Hall effects, the induced magnetic field and the viscous dissipation are neglected. Motivated by this fact, present study analyzes the effects of the solid volume fraction, types of nanoparticles, suction/blowing, magnetic field, permeability, radiation, Schmidt number and chemical reaction on velocity, temperature and concentration profiles.

This paper is organized as follows: In Section 2, the mathematical formulation of the MHD boundary layer stagnation flow and radiation heat transfer of a nanofluid with uniform suction or blowing through a porous medium past a flat plate is presented. Bernstein and orthonormal Bernstein polynomials and their properties are given in Section 3 and Section 4, respectively. After introducing a function approximation with exponential Bernstein functions in Section 5, a collocation method based on this approximation is proposed for solving the MHD flow in Section 6. The results and discussion for the all values of the relevant parameters are presented in Section 7. Finally a conclusion is drawn in Section 8.

## 2. Problem Statement and Mathematical Modelling

Consider a two-dimensional MHD boundary layer stagnation flow and radiation heat transfer of a nanofluid with uniform suction or blowing through a porous medium past a flat plate. The geometry and coordinate systems of the problem are shown in Fig. 1. The uniform magnetic field along the  $y$ -direction is  $B$  and the free stream velocity, the temperature at surface, the ambient temperature (far from the surface), the concentration near surface and the concentration in the free stream are assumed to be  $U$ ,  $T_w$ ,  $T_\infty$ ,  $C_w$ ,  $C_\infty$ , respectively.  $T_0$  is a constant measuring the rate of temperature increase along the sheet. It is assumed that there exists a first order chemical reaction effect and the fluid motion is based on Darcy's law, which accounts for the drag applied by the porous medium [31, 49]. Furthermore, It is supposed that the magnetic Reynolds number is small so that the thickness of the magnetic boundary-layer is large and induced magnetic field in comparison to the applied magnetic field, is insignificant. The viscous dissipation and Hall effects terms are also, neglected.

For the present problem, the steady boundary layer equations governing the nanofluid flow, radiation heat transfer and concentration fields can be written in dimensional form as proposed by Nield et al. [47] and Zhang et al. [57]

$$\frac{\partial u}{\partial x} + \frac{\partial v}{\partial y} = 0, \quad (1)$$

$$u \frac{\partial u}{\partial x} + v \frac{\partial u}{\partial y} = -\frac{1}{\rho_{nf}} \frac{\partial p}{\partial x} + \frac{\mu_{nf}}{\rho_{nf}} \frac{\partial^2 u}{\partial y^2} - \frac{\mu_{nf}}{\rho_{nf} k} u - \frac{\sigma_{nf} B^2}{\rho_{nf}} u, \quad (2)$$

$$u \frac{\partial T}{\partial x} + v \frac{\partial T}{\partial y} = \alpha_{nf} \frac{\partial^2 T}{\partial y^2} - \frac{1}{(\rho c_p)_{nf}} \frac{\partial q_r}{\partial y}, \quad (3)$$

$$u \frac{\partial C}{\partial x} + v \frac{\partial C}{\partial y} = D \frac{\partial^2 C}{\partial y^2} - K(C - C_\infty). \quad (4)$$

The corresponding boundary conditions are given by:

$$u = 0, \quad v = v_w, \quad T = T_w = T_\infty + T_0 \exp\left(\frac{x}{2L}\right), \quad (5)$$

$$C = C_w = C_\infty + C_0 \exp\left(\frac{x}{2L}\right), \quad y = 0,$$

$$u \rightarrow U = a \exp\left(\frac{x}{L}\right), \quad T \rightarrow T_\infty, \quad C \rightarrow C_\infty, \quad y \rightarrow \infty. \quad (6)$$

where  $u$  and  $v$  are the velocity components of the fluid along  $x$  and  $y$  directions, respectively,  $p$  is the fluid pressure,  $T$  is the temperature of the nanofluid,  $D$  is the mass diffusivity,  $U$  is the free-stream velocity,  $a$  is a constant number,  $\sigma_f$  and  $\sigma_{nf}$  are the electrical conductivity of the base fluid and the nanofluid.  $v_w(x) = v_0 \exp(x/2L)$  is a special suction or blowing velocity at the wall [8] with  $v_w(x) < 0$  for suction and  $v_w(x) > 0$  for injection,  $L$  is the reference length and  $v_0$  is a constant.  $K(x)$  is the variable reaction rate given by  $K(x) = K_0 \exp(x/L)$  [2] and  $K_0$  is a constant. Also,  $\rho_{nf}$  is the effective density of the nanofluid,  $\mu_{nf}$  is the effective viscosity of the nanofluid and  $\alpha_{nf}$  is the effective thermal diffusivity of the nanofluid [7, 38, 44, 45] satisfying

$$\begin{aligned} \rho_{nf} &= (1 - \phi)\rho_f + \phi\rho_s, \quad \mu_{nf} = \frac{\mu_f}{(1 - \phi)^{2.5}}, \quad \alpha_{nf} = \frac{k_{nf}}{(\rho c_p)_{nf}}, \\ (\rho c_p)_{nf} &= (1 - \phi)(\rho c_p)_f + \phi(\rho c_p)_s, \\ \frac{k_{nf}}{k_f} &= \frac{(k_s + 2k_f) - 2\phi(k_f - k_s)}{(k_s + 2k_f) + \phi(k_f - k_s)}, \\ \sigma_{nf} &= (1 - \phi)\sigma_f + \phi\sigma_s, \end{aligned} \quad (7)$$

where  $\phi$  is the nanoparticle volume fraction. In the free-stream, (2) becomes

$$U \frac{dU}{dx} = -\frac{1}{\rho_{nf}} \frac{\partial p}{\partial x} - \frac{\mu_{nf}}{\rho_{nf} K} U - \frac{\sigma_{nf} B^2}{\rho_{nf}} U. \quad (8)$$

Then, from (2) and (8), we can get

$$u \frac{\partial u}{\partial x} + v \frac{\partial u}{\partial y} = U \frac{dU}{dx} + \frac{\mu_{nf}}{\rho_{nf}} \frac{\partial^2 u}{\partial y^2} - \frac{\mu_{nf}}{\rho_{nf} k} (u - U) - \frac{\sigma_{nf} B^2}{\rho_{nf}} (u - U), \quad (9)$$

where  $c_p$  is the specific heat at constant pressure,  $B = B_0 \exp(x/2L)$ ,  $B_0$  is the externally imposed magnetic field in the  $y$ -direction [30],  $k = k_0 \exp(-x/L)$  is the non-uniform permeability of the medium and  $k_0$  is a constant which gives the initial permeability [43]. The radiative heat flux  $q_r$  is described by Rosseland's approximation for radiation [51] such that

$$q_r = -\frac{4\sigma_1}{3k_1} \frac{\partial T^4}{\partial y}, \quad (10)$$

where  $k_1$  and  $\sigma_1$  are the absorption coefficient and the Stefan-Boltzmann constant, respectively. We assume that the temperature differences within the flow are such that the term  $T^4$  may be expressed as a linear function of temperature. This is accomplished by expanding  $T^4$  in a Taylor series about a free stream temperature  $T_\infty$  as follows:

$$T^4 = T_\infty^4 + 4T_\infty^3(T - T_\infty) + 6T_\infty^2(T - T_\infty)^2 + \dots \quad (11)$$

Neglecting higher-order terms in the above equation beyond the first degree in  $(T - T_\infty)$ , we get  $T^4 \cong 4T_\infty^3 T - 3T_\infty^4$  and

$$\frac{\partial q_r}{\partial y} = -\frac{16\sigma_1 T_\infty^3}{3k_1} \frac{\partial^2 T}{\partial y^2}. \quad (12)$$

Then, equation (3) is reduced by using (12) as follows:

$$u \frac{\partial T}{\partial x} + v \frac{\partial T}{\partial y} = \alpha_{nf} \frac{\partial^2 T}{\partial y^2} + \frac{16\sigma_1 T_\infty^3}{3(\rho c_p)_{nf} k_1} \frac{\partial^2 T}{\partial y^2}. \quad (13)$$

Mandal and Mukhopadhyay [43] introduced the following similarity transformations

$$\begin{aligned} \eta &= y \sqrt{\frac{a}{2v_f L}} \exp\left(\frac{x}{2L}\right), \quad \psi = \sqrt{2aLv_f} f(\eta) \exp\left(\frac{x}{2L}\right), \\ \theta(\eta) &= \frac{T - T_\infty}{T_w - T_\infty}, \quad g(\eta) = \frac{C - C_\infty}{C_w - C_\infty}, \end{aligned} \quad (14)$$

where  $\psi(x, y)$  represent the stream function and is defined as  $u = \frac{\partial \psi}{\partial y}$ ,  $v = -\frac{\partial \psi}{\partial x}$ , so that equation (1) is satisfied identically. Substituting the

similarity transformations (14) into (4), (9) and (13), we obtain the following system of nonlinear ordinary differential equations:

$$\frac{1}{\phi_1} f''' + f f'' + 2(1 - f'^2) + \left( \frac{1}{\phi_1} P + \frac{\phi_4}{\phi_2} M \right) (1 - f') = 0, \quad (15)$$

$$\left[ \frac{k_{nf}}{\phi_3 k_f} + \frac{R}{\phi_3 k_f} \right] \theta'' + Pr(f\theta' - f'\theta) = 0, \quad (16)$$

$$g'' + Sc(fg' - f'g - \lambda g) = 0, \quad (17)$$

with boundary conditions

$$f = S, \quad f' = 0, \quad \theta = 1, \quad g = 1, \quad \eta = 0, \quad (18)$$

$$f' = 1, \quad \theta = 0, \quad g = 0 \quad \text{as } \eta \rightarrow \infty, \quad (19)$$

where  $P$  is permeability parameter,  $M$  is magnetic parameter,  $R$  is radiation parameter,  $S$  is suction/blowing parameter,  $Sc$  is Schmidt number,  $\lambda$  is chemical reaction parameter and  $Pr$  is the Prandtl number, which are defined as:

$$\begin{aligned} P &= \frac{2Lv_f}{ak_0}, \quad M = \frac{2\sigma_f B_0^2 L}{a\rho_f}, \quad R = \frac{16\sigma_1 T_\infty^3}{3k}, \\ S &= \frac{v_0}{\sqrt{av_f/2L}}, \quad Sc = \frac{v_f}{D}, \quad \lambda = \frac{K_0}{a}, \quad Pr = \frac{v_f}{\alpha_f}, \quad (20) \\ &\left\{ \begin{array}{l} \phi_1 = (1 - \phi)^{2.5} [(1 - \phi) + \phi\rho_s/\rho_f], \\ \phi_2 = (1 - \phi) + \phi\rho_s/\rho_f, \\ \phi_3 = (1 - \phi) + (\rho c_p)_s/(\rho c_p)_f, \\ \phi_4 = (1 - \phi) + \phi\sigma_s/\sigma_f. \end{array} \right. \end{aligned}$$

The physical quantities of interest in this study, are skin friction coefficient  $C_f$ , local Nusselt number  $Nu_x$  and local Sherwood number  $Sh_x$  are defined as [32]:

$$C_f = \frac{\tau_w}{\rho_f U^2}, \quad Nu_x = \frac{xq_w}{k_f(T_w - T_\infty)}, \quad Sh_x = \frac{x p_w}{D(C_w - C_\infty)}, \quad (21)$$

where  $\tau_w$  is the skin friction,  $q_w$  is the heat flux from the sheet and  $p_w$  is the mass flux at the wall surface, which are given by:

$$\tau_w = \mu_{nf} \frac{\partial u}{\partial y} \Big|_{y=0}, \quad q_w = -k_{nf} \frac{\partial T}{\partial y} \Big|_{y=0}, \quad p_w = -D \frac{\partial C}{\partial y} \Big|_{y=0}. \quad (22)$$

By substituting (22) into (21), we have:

$$\begin{aligned} (2L/x)(1 - \phi)^{2.5}C_f Re_x^{1/2} = f''(0), \quad Nu_x Re_x^{-1/2}(k_f/k_{nf}) = -\theta'(0), \\ Sh_x Re_x^{-1/2} = -g'(0), \end{aligned} \tag{23}$$

where  $Re_x = Ux^2/(2Lv_f)$  is the local Reynolds number.

In view of the present work, the fluid is a water based nanofluid containing three different types of nanoparticles; copper, aluminium oxide and silver nanoparticles. The thermophysical properties of the nanofluids are displayed in Table 1.

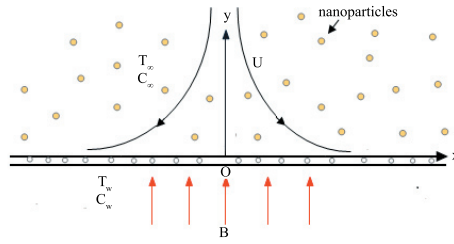


**Figure 1.** Level plate in a porous medium saturated with a fluid with nanoparticles in suspension

### 3. Bernstein Polynomials and Their Properties

Bernstein polynomials have important applications in computer graphics and have been applied for approximations of functions in many areas of mathematics and other fields such as smoothing in statistics and constructing Bézier curves [19, 23, 33]. Bernstein polynomials of the degree  $n$  are defined on the interval  $[a, b]$  as [10]

$$B_{i,n}(x) = \binom{n}{i} \frac{(x - a)^i (b - x)^{n-i}}{(b - a)^n}, \quad 0 \leq i \leq n, \tag{24}$$

where the binomial coefficients are calculated by  $\binom{n}{i} = \frac{n!}{i!(n-i)!}$ . The properties of Bernstein polynomials have been investigated by many authors some of which to be mentioned briefly here.

These Bernstein polynomials form a basis on  $[a, b]$  and there are  $n + 1$ ,  $n$ th-degree polynomials. If  $i < 0$  or  $i > n$  we set  $B_{i,n}(x) = 0$ . Also for all

$i = 0, 1, \dots, n$  and all  $x$  in  $[a, b]$ , we have  $B_{i,n}(x) \geq 0$ . In addition, these polynomials can be generated by a recursive definition over the interval  $[a, b]$  as follows:

$$B_{i,n}(x) = \frac{b-x}{b-a}B_{i,n-1}(x) + \frac{x-a}{b-a}B_{i-1,n-1}(x). \quad (25)$$

The binomial expansion of the right-hand side of the equality  $(b-a)^n = ((x-a) + (b-x))^n$  shows that the sum of all Bernstein polynomials of the degree  $n$  is the constant 1, i.e.,  $\sum_{i=0}^n B_{i,n}(x) = 1$ . One of the benefits of the Bernstein polynomial approximation of a continuous function  $f$  is that it approximates  $f$  on  $[a, b]$  using only the values of  $f$  at  $x_i = a + (b-a)i/n$ ,  $i = 0, 1, \dots, n$ , that is,

$$f(x) \simeq \mathbb{B}_n f(x) = \sum_{i=0}^n f(x_i)B_{i,n}(x).$$

The above approximation is preferred when the evaluation of  $f$  is difficult, expensive and time consuming.

An explicit expression for the derivatives of Bernstein polynomials of any degree and any order in terms of Bernstein polynomials on  $[0, 1]$ , introduced by Doha et al. [17] is as follows:

$$\frac{d^k}{dx^k} B_{i,n}(x) = \frac{n!}{(n-k)!} \sum_{j=\max\{0, i+k-n\}}^{\min\{i, k\}} (-1)^{j+k} \binom{k}{j} B_{i-j, n-k}(x). \quad (26)$$

It can easily be shown that for Bernstein polynomials on  $[a, b]$  [23, 28]:

$$\frac{d^k}{dx^k} B_{i,n}(x) = \frac{n!}{(b-a)^k (n-k)!} \sum_{j=\max\{0, i+k-n\}}^{\min\{i, k\}} (-1)^{j+k} \binom{k}{j} B_{i-j, n-k}(x). \quad (27)$$

The product of two Bernstein polynomials is also a Bernstein polynomial which is given by:

$$B_{i,j}(x)B_{k,m}(x) = \frac{\binom{j}{i}\binom{m}{k}}{\binom{j+m}{i+k}} B_{i+k, j+m}(x). \quad (28)$$

All Bernstein polynomials of the same order have the same definite integral over the interval  $[a, b]$ , namely

$$\int_a^b B_{i,n}(x)dx = \frac{b-a}{n+1}. \quad (29)$$

The definite integrals of the products of Bernstein polynomials can be found using (28) and (29), as follows:

$$\int_a^b B_{k,n}(x)B_{i,n}(x)dx = \frac{\binom{n}{k}\binom{n}{i}}{(2n+1)\binom{2n}{k+i}}(b-a). \quad (30)$$

**Table 1:** Thermophysical properties of the base fluid and nanoparticles

| Physical properties         | Fluid phase (water)  | Cu                 | Al <sub>2</sub> O <sub>3</sub> | Ag                  |
|-----------------------------|----------------------|--------------------|--------------------------------|---------------------|
| $c_p$ (J/kgK)               | 4179                 | 385                | 765                            | 235                 |
| $\rho$ (kg/m <sup>3</sup> ) | 997.1                | 8933               | 3970                           | 10.50               |
| $k$ (W/mK)                  | 0.613                | 400                | 40                             | 429                 |
| $\sigma$ (S/m)              | $5.5 \times 10^{-6}$ | $59.6 \times 10^6$ | $35 \times 10^6$               | $63.01 \times 10^6$ |

## 4. Orthonormal Bernstein Polynomials

The explicit representation of the orthonormal Bernstein polynomials of  $n$ th degree are defined on the interval  $[0, 1]$  as follows [5]:

$$\mathfrak{B}_{i,n}(x) = \left(\sqrt{2(n-i)+1}\right) (1-x)^{n-i} \sum_{j=0}^i (-1)^j \binom{2n+1-j}{i-j} \binom{i}{j} x^{i-j}. \quad (31)$$

Moreover, using (24) on the interval  $[0, 1]$ , (31) can be written in a simpler form in terms of the non-orthonormal Bernstein basis functions as [5]:

$$\mathfrak{B}_{i,n}(x) = \left(\sqrt{2(n-i)+1}\right) \sum_{j=0}^i (-1)^j \frac{\binom{2n+1-j}{i-j} \binom{i}{j}}{\binom{n-j}{i-j}} B_{i-j,n-j}(x). \quad (32)$$

By changing the variable  $x = (t-a)/(b-a)$ , we will have the orthonormal Bernstein polynomials on the arbitrary interval  $[a, b]$  as:

$$\mathfrak{B}_{i,n}(t) = \left(\sqrt{\frac{2(n-i)+1}{b-a}}\right) \sum_{j=0}^i (-1)^j \frac{\binom{2n+1-j}{i-j} \binom{i}{j}}{\binom{n-j}{i-j}} B_{i-j,n-j}\left(\frac{t-a}{b-a}\right). \quad (33)$$

The orthonormal Bernstein polynomial,  $\mathfrak{B}_{j,n}(x)$  on  $[0, 1]$  is the  $n$ th eigenfunction of the singular Sturm-Liouville problem [5]:

$$\frac{d}{dx} \left[ x(1-x)^2 \frac{d\mathfrak{B}(x)}{dx} \right] + n(n+2)(1-x)\mathfrak{B}(x) + (n-j+1)(j-n)\mathfrak{B}(x) = 0, \quad (34)$$

with the orthogonality property:

$$\int_0^1 \mathfrak{B}_{i,n}(x)\mathfrak{B}_{j,n}(x)dx = \delta_{ij}. \quad (35)$$

Also, using (33) and (30), the orthonormal polynomials necessarily satisfy the following relationships over the interval  $[0, 1]$ :

$$\int_0^1 \mathfrak{B}_{i,n}(x)B_{j,n}(x)dx = \begin{cases} \sqrt{2(n-i)+1} \sum_{k=0}^i (-1)^k \frac{\binom{2n+1-k}{i-k} \binom{i}{k} \binom{n}{j}}{[2n+1-k] \binom{2n-k}{i+j-k}}, & j \geq i, \\ 0, & j < i. \end{cases} \quad (36)$$

In the end of this section, we will prove the following theorem, for the derivatives of  $\mathfrak{B}_{i,n}(x)$  at the end points of the interval  $[a, b]$ .

**Theorem 4.1.** [27, 26] For  $k = 0, 1, \dots, n$ , we have

$$\frac{d^k}{dx^k} \mathfrak{B}_{i,n}(a) = \sqrt{\frac{2(n-i)+1}{(b-a)^{2k+1}}} \sum_{j=0}^i \frac{(-1)^{i+k} \binom{2n+1-j}{i-j} \binom{i}{j} \binom{k}{i-j} (n-j)!}{\binom{n-j}{i-j} (n-j-k)!} \gamma_{i-j,k}, \quad (37)$$

and

$$\frac{d^k}{dx^k} \mathfrak{B}_{i,n}(b) = \sqrt{\frac{2(n-i)+1}{(b-a)^{2k+1}}} \sum_{j=0}^i \frac{(-1)^{n-i+j} \binom{2n+1-j}{i-j} \binom{i}{j} \binom{k}{n-i} (n-j)!}{\binom{n-j}{i-j} (n-j-k)!} \gamma_{n-i,k}, \quad (38)$$

where

$$\gamma_{i,k} = \begin{cases} 1, & i \leq k, \\ 0, & i > k. \end{cases} \quad (39)$$

## 5. Exponential Bernstein Functions (EBFs)

The main objective of this section is to describe the exponential Bernstein functions (EBFs) and express some of their basic properties for approximation on the half line.

## 5.1 Basic properties

According to Sections 3 and 4, the basic properties of Bernstein and orthogonal Bernstein polynomials are derived in the finite domain  $[a, b]$ , but the problem of MHD flow and radiation heat transfer of nanofluids in porous media with variable surface heat flux and chemical reaction is defined on the semi-infinite domain  $[0, +\infty)$ . The use of a suitable mapping to transfer semi-infinite domain  $[0, +\infty)$  to the finite domain  $[a, b]$  is a common and effective strategy to construct approximations on the half line.

So, we define the exponential Bernstein functions (EBFs) of order  $n$  as follows:

$$\mathbf{EB}_{i,n}(x; l) = \mathfrak{B}_{i,n}(x) \circ \Phi_l(x) = \mathfrak{B}_{i,n}(\Phi_l(x)), \quad i = 0, 1, \dots, n, \quad (40)$$

where  $\Phi_l = [0, +\infty) \rightarrow [a, b]$  is an exponential mapping given by

$$\Phi_l(x) = b + (a - b) \exp\left(-\frac{x}{l}\right), \quad (41)$$

and  $l$  is a positive scaling/stretching factor. The inverse mapping of  $y = \Phi_l(x)$  is

$$x = \Phi_l^{-1}(y) = l \ln\left(\frac{b - a}{b - y}\right). \quad (42)$$

Furthermore, we can find the inverse image of the spaced nodes  $\{y_j\}_{j=0}^n \subset [a, b]$  as

$$x_j^l = \Phi_l^{-1}(y_j) = l \ln\left(\frac{b - a}{b - y_j}\right), \quad j = 0, 1, \dots, n. \quad (43)$$

We need to choose the parameter  $l$  so that controls the width of the basis functions. Although, some methods for making this choice suggested in [11, 12], but there is not a general method for this choose and its selected usually by trial and error.

**Theorem 5.1.1.** *Let  $a = 0$  and  $b = 1$ , then the exponential Bernstein functions  $\mathbf{EB}_{j,n}(y; l)$  on  $[0, \infty)$  are the eigenfunctions of the singular*

*Sturm-Liouville problem:*

$$l \left[ \left( 2 \exp \left( -\frac{y}{l} \right) - 1 \right) \frac{dp}{dy} + l \left( 1 - \exp \left( -\frac{y}{l} \right) \right) \frac{d^2p}{dy^2} \right] + n(n+2) \exp \left( -\frac{y}{l} \right) p + \gamma_{j,n} p = 0, \quad (44)$$

where  $\gamma_{j,n} = (n-j+1)(j-n)$ ,  $j = 0, 1, \dots, n$ .

**Proof.** As mentioned in Section 4,  $\mathfrak{B}_{j,n}(x)$  on  $[0, 1]$  is the  $n$ th eigenfunction of the singular Sturm-Liouville problem (34). Let

$$p(y) = \mathfrak{B}_{j,n} \left( 1 - \exp \left( -\frac{y}{l} \right) \right). \quad (45)$$

Now by using the following transformations

$$x = 1 - \exp \left( -\frac{y}{l} \right), \quad y = l \ln \left( \frac{1}{1-x} \right), \quad x \in [0, 1), \quad y \in [0, \infty), \quad (46)$$

we can get

$$\frac{d\mathfrak{B}_{j,n}(x)}{dx} = \left( \frac{l}{1-x} \right) \frac{dp}{dy}, \quad \frac{d}{dx} \left( \frac{dp}{dy} \right) = \left( \frac{l}{1-x} \right) \frac{d^2p}{dy^2}. \quad (47)$$

Inserting (47) into (34), yields

$$l \left[ (1-2x) \frac{dp}{dy} + xl \frac{d^2p}{dy^2} \right] + n(n+2)(1-x) \frac{dp}{dy} + \gamma_{j,n} p(y) = 0, \quad (48)$$

where  $\gamma_{j,n} = (n-j+1)(j-n)$ ,  $j = 0, 1, \dots, n$ . Consequently, from (46) and (48), the Sturm-Liouville problem for exponential Bernstein functions can be derived as (44).  $\square$

**Lemma 5.1.2.** *For  $i = 0, 1, \dots, n$ , we have*

$$\begin{aligned}
 1) \quad \mathbf{EB}_{i,n}(0; l) &= (-1)^i \sqrt{\frac{2(n-i)+1}{b-a}}, \\
 2) \quad \lim_{x \rightarrow +\infty} \mathbf{EB}_{i,n}(x; l) &= \begin{cases} 0, & 0 \leq i \leq n-1, \\ \frac{1}{\sqrt{b-a}} \sum_{j=0}^n (-1)^j \binom{2n+1-j}{n-j} \binom{n}{j}, & i = n, \end{cases} \\
 3) \quad \mathbf{EB}'_{i,n}(0; l) &= \left( \sqrt{\frac{2(n-i)+1}{l^2(b-a)}} \right) (-1)^{i+1} (-i^2 + 2in + i + n), \\
 4) \quad \lim_{x \rightarrow +\infty} \mathbf{EB}'_{i,n}(x; l) &= 0.
 \end{aligned}$$

**Proof.** From (40), we have

$$\mathbf{EB}_{i,n}(x; l) = \mathfrak{B}_{i,n}(\Phi_l(x)), \quad \mathbf{EB}'_{i,n}(x; l) = \Phi'_l(x) \mathfrak{B}'_{i,n}(\Phi_l(x)). \quad (49)$$

In addition, from (41) it follows that

$$\Phi_l(0) = a, \quad \lim_{x \rightarrow +\infty} \Phi_l(x) = b, \quad \Phi'_l(0) = \frac{b-a}{l}, \quad \lim_{x \rightarrow +\infty} \Phi'_l(x) = 0. \quad (50)$$

Now, by applying Theorem 4.1 in the special cases  $k = 0$  and  $k = 1$ , the lemma can be proved.  $\square$

## 5.2 Function approximation

Let us denote  $\Lambda = [0, +\infty)$ . We determine  $w(x) = \frac{b-a}{l} \exp(-\frac{x}{l})$  as a non-negative, integrable and real-valued weight function for the exponential Bernstein functions over the interval  $[0, +\infty)$ . We define

$$L_w^2(\Lambda) = \{f | f \text{ is measurable on } \Lambda \text{ and } \|f\|_w < \infty\}, \quad (51)$$

equipped with the following inner product and norm

$$\langle f, g \rangle_w = \int_{\Lambda} f(x)g(x)w(x)dx, \quad \|f\|_w = \langle f, f \rangle_w^{\frac{1}{2}}. \quad (52)$$

Let  $y = \Phi_l(x)$ , then we have

$$\frac{dy}{dx} = \frac{b-a}{l} \exp\left(-\frac{x}{l}\right), \quad \frac{dx}{dy} = \frac{l}{b-y}, \quad w(x) \frac{dx}{dy} = 1. \quad (53)$$

Hence, the orthogonality relation (35) leads to

$$\langle \mathbf{EB}_{i,n}(x;l), \mathbf{EB}_{j,n}(x;l) \rangle_w = \delta_{ij}. \quad (54)$$

Suppose that  $H = L_w^2(\Lambda)$ , and let  $\{\mathbf{EB}_{0,n}(x;l), \mathbf{EB}_{1,n}(x;l), \dots, \mathbf{EB}_{n,n}(x;l)\} \subset H$  be the set of exponential orthonormal Bernstein functions of the order  $n$ . Also, we define  $P_n^l : L_w^2(\Lambda) \longrightarrow \mathfrak{EB}_n^l$  by

$$P_n^l f(x) = \sum_{i=0}^n f_i \mathbf{EB}_{i,n}(x;l), \quad (55)$$

where

$$\mathfrak{EB}_n^l = \text{Span}\{\mathbf{EB}_{0,n}(x;l), \mathbf{EB}_{1,n}(x;l), \dots, \mathbf{EB}_{n,n}(x;l)\}. \quad (56)$$

**Theorem 5.2.1.** [34] *For every given  $f$  in a Hilbert space  $H$  and every given closed subspace  $Z$  of  $H$  there is a unique best approximation to  $w$  from  $Z$ .*

Since  $H = L_w^2(\Lambda)$  is Hilbert space and  $\mathfrak{EB}_n^l$  is a finite-dimensional subspace and  $\mathfrak{EB}_n^l$  is a closed subspace of  $H$ , therefore,  $\mathfrak{EB}_n^l$  is a complete subspace of  $H$ . So, if  $f$  be an arbitrary element in  $H$ , by Theorem 5.2.1,  $f$  has the unique best approximation from  $\mathfrak{EB}_n^l$  such as  $f^*$ , that is

$$\exists f^* \in \mathfrak{EB}_n^l; \quad \forall g \in \mathfrak{EB}_n^l \quad \|f - f^*\|_w \leq \|f - g\|_w. \quad (57)$$

Since  $f^* \in \mathfrak{EB}_n^l$ , there exist the unique coefficients  $f_0, f_1, \dots, f_n$  such that

$$f(x) \simeq f^*(x) = \sum_{i=0}^n f_i \mathbf{EB}_{i,n}(x;l), \quad (58)$$

where the coefficients  $f_i$  can be obtained by

$$f_i = \langle f(x), \mathbf{EB}_{j,n}(x;l) \rangle_w, \quad i = 0, 1, \dots, n. \quad (59)$$

## 6. Exponential Bernstein Collocation Method (EBCM)

In this section, we use the exponential Bernstein collocation method (EBCM) to find solutions of MHD flow and radiative heat transfer of a nanofluid against a flat plate in porous media with variable wall temperature and a first-order chemical reaction.

Consider the system of nonlinear ordinary differential equations (15)-(17) with boundary conditions (18) and (19) to determine the approximate solutions of  $f(\eta)$ ,  $\theta(\eta)$  and  $g(\eta)$ .

At first, we approximate function  $f(\eta)$  by  $(n_f + 1)$  terms of exponential Bernstein functions as

$$f(\eta) \simeq P_{n_f}^{l_f} f(\eta) = \sum_{i=0}^{n_f} f_i \mathbf{EB}_{i,n_f}(\eta; l_f). \quad (60)$$

But, from fourth part of Lemma 5.1.2, we have

$$\lim_{\eta \rightarrow +\infty} \frac{dP_{n_f}^{l_f} f(\eta)}{d\eta} = \sum_{i=0}^{n_f} f_i \left( \lim_{\eta \rightarrow +\infty} \mathbf{EB}'_{i,n_f}(\eta; l_f) \right) = 0. \quad (61)$$

It means that  $f'(\infty) = 0$  and the boundary condition  $f'(\infty) = 1$  does not satisfy. To establish this condition, we approximate function  $f(\eta)$  as:

$$f(\eta) \simeq \widehat{P}_{n_f}^{l_f} f(\eta) = \eta + P_{n_f}^{l_f} f(\eta) = \eta + \sum_{i=0}^{n_f} f_i \mathbf{EB}_{i,n_f}(\eta; l_f). \quad (62)$$

Now we have

$$\lim_{\eta \rightarrow +\infty} \frac{d\widehat{P}_{n_f}^{l_f} f(\eta)}{d\eta} = 1, \quad (63)$$

and therefore the first boundary condition (19) is satisfied. We construct the residual function  $RES_f(\eta)$  by substituting  $f(\eta)$  by  $\widehat{P}_{n_f}^{l_f} f(\eta)$  in (15) as:

$$\begin{aligned}
 RES_f(\eta) &= \frac{1}{\phi_1} \frac{d^3 \widehat{P}_{n_f}^{l_f} f(\eta)}{d\eta^3} + \widehat{P}_{n_f}^{l_f} f(\eta) \frac{d^2 \widehat{P}_{n_f}^{l_f} f(\eta)}{d\eta^2} + \\
 &+ 2 \left( 1 - \left( \frac{d \widehat{P}_{n_f}^{l_f} f(\eta)}{d\eta} \right)^2 \right) + \left( \frac{1}{\phi_1} P + \frac{\phi_4}{\phi_2} M \right) \left( 1 - \frac{d \widehat{P}_{n_f}^{l_f} f(\eta)}{d\eta} \right) = 0. \quad (64)
 \end{aligned}$$

Let

$$t_j = -\cos \left( \frac{2j\pi}{2n+1} \right), \quad j = 0, 1, \dots, n, \quad (65)$$

are the  $(n+1)$  Chebyshev-Gauss-Radau points. From (42), we define the collocation points  $\eta_j^{l_f} \in [0, +\infty)$  as follows:

$$\eta_j^{l_f} = \Phi_{l_f}^{-1}(t_j) = l_f \ln \left( \frac{2}{1-t_j} \right), \quad j = 0, 1, \dots, n. \quad (66)$$

The equations for obtaining the coefficients  $f_i$ s come from equalizing  $RES_f(\eta)$  to zero at collocation points  $\{\eta_j^{l_f}\}_{j=0}^{n_f-2}$  plus two boundary conditions as follows:

$$RES_f(\eta_j^{l_f}) = 0, \quad j = 0, 1, \dots, n_f - 2, \quad (67)$$

$$\widehat{P}_{n_f}^{l_f} f(\eta_0^{l_f}) = S, \quad \left. \frac{d \widehat{P}_{n_f}^{l_f} f(\eta)}{d\eta} \right|_{\eta=\eta_0^{l_f}} = 0. \quad (68)$$

We can rewrite the boundary conditions (68) by the first and third parts of Lemma 5.1.2 as:

$$\sum_{i=0}^{n_f} f_i \zeta_i = S, \quad \sum_{i=0}^{n_f} f_i \tilde{\zeta}_i = 0, \quad (69)$$

where

$$\begin{aligned}
 \zeta_i &= (-1)^i \sqrt{\frac{2(n-i)+1}{b-a}}, \\
 \tilde{\zeta}_i &= \left( \sqrt{\frac{2(n-i)+1}{l^2(b-a)}} \right) (-1)^{i+1} (-i^2 + 2in + i + n).
 \end{aligned}$$

Equations (67) and (69) generate a set of  $(n_f + 1)$  nonlinear equations that can be solved by Newton method for the unknown coefficients  $f_i$ s. Now, by finding the approximate solutions  $\widehat{P}_{n_f}^{l_f} f(\eta)$ , we suppose that the approximate solutions  $\theta(\eta)$  and  $g(\eta)$  of (16) and (17) are as follows:

$$g(\eta) \simeq P_{n_g}^{l_g} g(\eta) = \sum_{i=0}^{n_g} g_i \mathbf{EB}_{i,n_g}(\eta; l_g), \quad (70)$$

$$\theta(\eta) \simeq P_{n_\theta}^{l_\theta} \theta(\eta) = \sum_{i=0}^{n_\theta} \theta_i \mathbf{EB}_{i,n_\theta}(\eta; l_\theta). \quad (71)$$

Similarly, we make the residual functions  $RES_\theta(\eta)$  and  $RES_g(\eta)$  by substituting  $P_{n_g}^{l_g} g(\eta)$  and  $P_{n_\theta}^{l_\theta} \theta(\eta)$  in equations (16) and (17) as:

$$\begin{aligned} RES_\theta(\eta) = & \left[ \frac{k_{nf}}{\phi_3 k_f} + \frac{R}{\phi_3 k_f} \right] \frac{d^2 P_{n_\theta}^{l_\theta} \theta(\eta)}{d\eta^2} + \\ & + Pr \left( \widehat{P}_{n_f}^{l_f} f(\eta) \frac{dP_{n_\theta}^{l_\theta} \theta(\eta)}{d\eta} - \frac{d\widehat{P}_{n_f}^{l_f} f(\eta)}{d\eta} P_{n_\theta}^{l_\theta} \theta(\eta) \right) = 0, \end{aligned} \quad (72)$$

$$\begin{aligned} RES_g(\eta) = & \frac{d^2 P_{n_g}^{l_g} g(\eta)}{d\eta^2} + \\ & + Sc \left( \widehat{P}_{n_f}^{l_f} f(\eta) \frac{dP_{n_g}^{l_g} g(\eta)}{d\eta} - \frac{d\widehat{P}_{n_f}^{l_f} f(\eta)}{d\eta} P_{n_g}^{l_g} g(\eta) - \lambda P_{n_g}^{l_g} g(\eta) \right) = 0. \end{aligned} \quad (73)$$

Using the collocation points (66), the equations for obtaining the coefficients  $\theta_i$ s and  $g_i$ s come through equalizing  $RES_\theta(\eta)$  and  $RES_g(\eta)$  to zero at these points plus four boundary conditions as follows:

$$RES_\theta(\eta_j^{l_\theta}) = 0, \quad j = 0, 1, \dots, n_\theta - 2, \quad (74)$$

$$RES_g(\eta_j^{l_g}) = 0, \quad j = 0, 1, \dots, n_g - 2, \quad (75)$$

$$P_{n_\theta}^{l_\theta} \theta(\eta_0^{l_\theta}) = 1, \quad \lim_{\eta \rightarrow +\infty} P_{n_\theta}^{l_\theta} \theta(\eta) = 0, \quad (76)$$

$$P_{n_g}^{l_g} g(\eta_0^{l_g}) = 1, \quad \lim_{\eta \rightarrow +\infty} P_{n_g}^{l_g} g(\eta) = 0. \quad (77)$$

Again, by the first two parts of Lemma 5.1.2, we rewrite the boundary

conditions (76) and (77) as follows:

$$\sum_{i=0}^{n_\theta} \theta_i \zeta_i = 1, \quad \theta_{n_\theta} = 0, \quad (78)$$

$$\sum_{i=0}^{n_g} g_i \zeta_i = 1, \quad g_{n_g} = 0. \quad (79)$$

Equations (74), (75), (78) and (79) generate a set of  $(n_\theta + 1) \times (n_g + 1)$  nonlinear equations that can be solved by Newton method for the unknown coefficients  $g_i$ s and  $\theta_i$ s.

## 7. Results and Discussion

In this section, we present the numerical results of the EBCM to solve the system of nonlinear ordinary differential equations (15)-(17) subject to boundary conditions (18) and (19). Graphical and tabulated results are presented to see the influence of the solid volume fraction, types of nanoparticles, suction/blowing, magnetic field, permeability radiation, Schmidt number and chemical reaction on the velocity, temperature and concentration profiles. Furthermore, the friction factor, local Nusselt number and local Sherwood number are discussed and presented through tables and graphs. To illustrate the reliability of the proposed method, we compare the numerical results of EBFM with the DTM-BF method [57] and numerical method (based on fourth-order RungeKutta method and shooting method). Here, for graphical results, we consider  $Pr = 6.2$  and nanoparticle volume fraction in the range of  $0 \leq \phi \leq 0.2$  as mentioned in [48]. Also, all the EBCM results in this section are computed using  $n_f = n_\theta = n_g = 30$ ,  $l_f = 3$  and  $l_\theta = l_g = 2$ .

Fig. 2 reveals the velocity, temperature and concentration distributions of Cu-water nanofluid for different values of the nanoparticle volume fraction  $\phi$ . It is clearly observed that the velocity and temperature profiles increase with increasing the value of  $\phi$ , whereas the concentration thickness decreases. The effect of  $\phi$  on the concentration in contrast to velocity and temperature is far less clear. Also, it can be concluded that

the thermal conductivity and thickness of thermal boundary layer of nanofluid are increasing with an increase in  $\phi$ .

The velocity, temperature and concentration profiles for various types of the nanoparticles are depicted in Fig. 3. It is evident that, contrary to temperature and concentration, the Cu-water nanofluid has the higher velocity rates as compared to other nanofluids.

In order to survey the accuracy of the present method, the residual errors (64), (72) and (73) for different nanofluid and nanoparticle volume fraction are illustrated in Fig.s 4 and 5.

Fig. 6 illustrates the effect of suction/blowing parameter  $S$  on the velocity, temperature and concentration profiles for Cu-water nanofluid. For the wall suction ( $S > 0$ ), the boundary layer thickness decreases and the fluid velocity increases. In Fig. 6,  $S = 0$  indicates the non-porous plate and it is clear that for blowing ( $S < 0$ ), the fluid velocity decreases. Also, it is seen that temperature distribution, concentration and thickness of concentration boundary layer reduced by an increase in the suction/blowing parameter  $S$ .

The influence of magnetic field parameter  $M$  on the velocity, temperature and concentration for Cu-water nanofluid is shown in Fig. 7. It is observed that with increasing of  $M$  the velocity increases and the thickness of velocity boundary decreases. Moreover, it is clear that the influence of  $M$  on the temperature and concentration are not significant.

The effects of permeability parameter  $P$  on the fluid velocity, temperature and concentration for Cu-water are demonstrated in Fig. 8. As seen in this figure, increasing in the  $P$  makes an increase in the velocity profile and also has a decreasing effect on the temperature and concentration profiles, but the changes in the temperature and concentration profiles are not very sensitive.

Fig. 9 illustrates the effect of the thermal radiation parameter  $R$  on the temperature distribution for Cu-water nanofluid. It is obvious that with increasing of  $R$  the thermal boundary layer thickness of the flow increases.

Fig. 10 represents the effect of Schmidt number  $Sc$  on the concentration

profiles of the flow. According to this figure the concentration and the thickness of boundary layer decrease by increasing of  $Sc$ .

The influence of the chemical reaction coefficient  $\lambda$  on the concentration profiles is shown in Fig. 11. It can be seen that the concentration and the thickness of concentration boundary layer of the nanofluids decrease with increasing the value of  $\lambda$ .

From equations (15)-(17), it is clearly observed that the thermal radiation on the velocity and concentration, chemical reaction and Schmidt number on the velocity and temperature do not show any influence.

Tables 2 and 3 display the influence of the governing parameters on the heat transfer and mass transfer coefficients for Cu-water,  $Al_2O_3$ -water and Ag-water nanofluids. The tables also provide a comparison between the presented method, numerical method based on fourth-order RungeKutta method and shooting method, and the DTM-BF method [57]. From the Table 2, it can be seen that increase in  $R$  and  $\phi$  declines the heat transfer coefficients. Table 3 shows that, the mass transfer coefficients increases by increasing the  $Sc$  parameter while an increase in  $\phi$  has slight effect on the mass transfer coefficients.

Fig. 12 shows the graphical representations for the various nanoparticles on the skin friction, local Nusselt number and local Sherwood number, respectively. From Fig. 12(a), it can be seen that skin friction coefficient is to increase with the increase of  $\phi$  for Cu-water nanofluid. Increasing the nanoparticle volume fraction decreases the skin friction coefficient for Ag-water nanoparticle. An enhancement in  $\phi$  have a negligible effect in the skin friction of  $Al_2O_3$ -water. The variation of local Nusselt number for different values of  $\phi$  is shown in Fig. 12(b). It is observed that an increase in the value of nanoparticle volume fraction parameter decreases the local Nusselt number of the three nanoparticles Cu,  $Al_2O_3$  and Ag. Fig. 12(c) shows that local Sherwood number has slight changes for different values of nanoparticle volume fraction parameter. Nevertheless, for Cu-water, local Sherwood number grows when the  $\phi$  is increased. Nanoparticle volume fraction parameter declines the local Sherwood number of the Ag-water nanofluid. The local Sherwood number has slight change for  $Al_2O_3$ -water with the increase in  $\phi$ .

The effects of the suction/blowing parameter, the magnetic parameter and the permeability parameter on local Nusselt and Sherwood numbers are displayed in Fig. 13. For all nanofluid, the local Nusselt and Sherwood number are an increasing function of each of the suction/blowing parameter, the magnetic parameter and the permeability parameter.

The effects of the suction/blowing parameter and the volume fraction of nanofluid on the Nusselt and Sherwood number are shown in Figs. 14. For a fixed value of  $S$ , the Nusselt and Sherwood number have slight change for different values of  $\phi$ .

## 8. Conclusions

In this study, the MHD flow and radiation heat transfer of nanofluid against a flat plate in porous medium with variable surface heat flux and chemical reaction was investigated using the exponential Bernstein collocation method (EBCM). The difficulty in this type of problems, due to the existence of its boundary condition in the infinity, is overcome here. The effects of various parameters on the velocity, temperature and concentration distribution are discussed with the help of graphs for Cu-water,  $\text{Al}_2\text{O}_3$ -water and Ag-water nanofluids. The influence of the nanoparticle volume fraction parameters on the skin friction, local Nusselt number and local Sherwood number is also examined. The results obtained from EBCM are in excellent agreement with those obtained from numerical solutions by fourth-order Runge-Kutta method and DTM-BF method [57]. It is worth noting that the proposed method in the current paper can be extended to solve similar nonlinear problems in fluid mechanics.

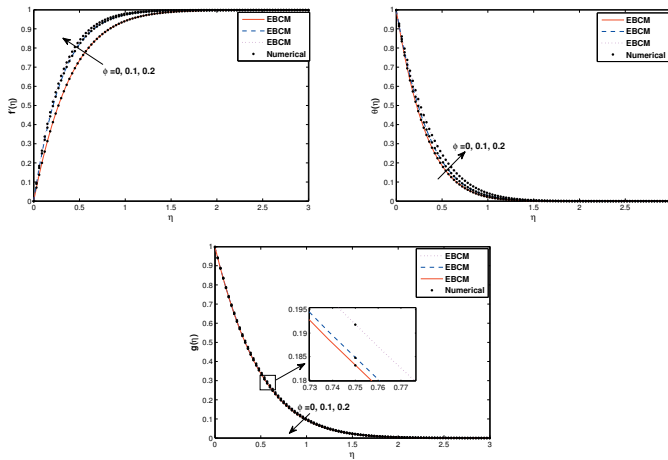


**Figure 2.** Effect of the  $\phi$  on the velocity, temperature and concentration profiles for Cu-water nanofluid with  $P = 0.5, R = S = 1, M = 10^{-12}, Sc = \lambda = 1$

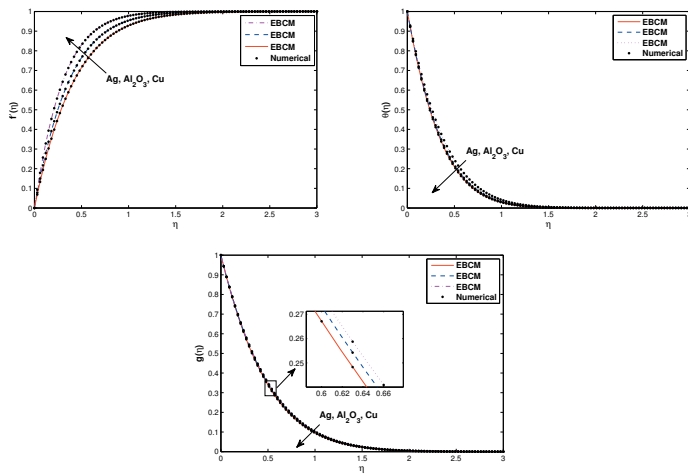


**Figure 3.** Effect of types of the nanofluids on the velocity, temperature and concentration profiles with  $P = S = 1, R = 1, M = 10^{-12}, \phi = 0.1, Sc = \lambda = 1$ .

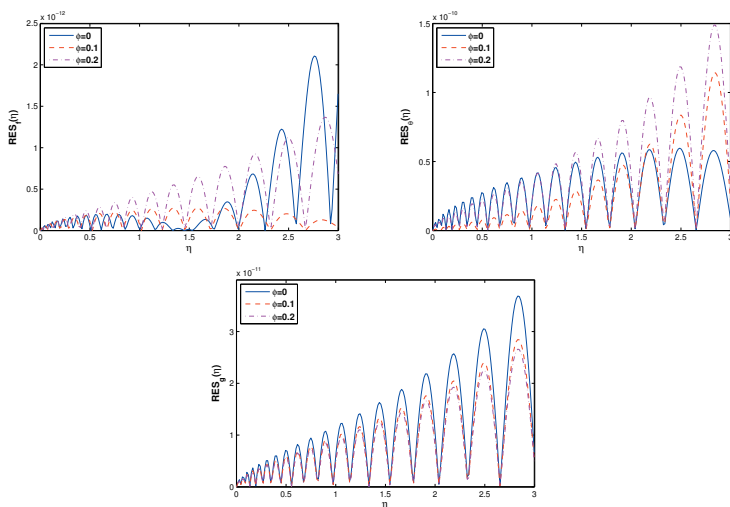


**Figure 4.** Absolute of the  $RES_f(\eta)$ ,  $RES_\theta(\eta)$  and  $RES_g(\eta)$  for the different values  $\phi$  with  $P = 0.5, R = S = 1, M = 10^{-12}, Sc = \lambda = 1$ .

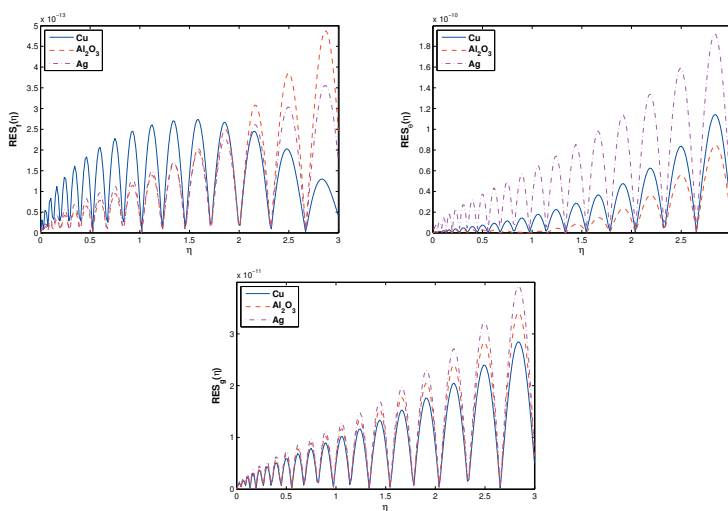


**Figure 5.** Absolute of the  $RES_f(\eta)$ ,  $RES_\theta(\eta)$  and  $RES_g(\eta)$  for the different nanofluid with  $P = S = 1, R = 1, M = 10^{-12}, \phi = 0.1, Sc = \lambda = 1$ .

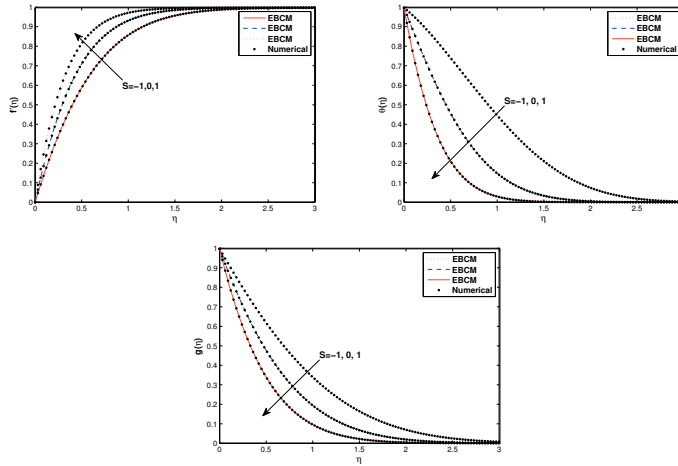


**Figure 6.** Effect of the suction/blowing parameter  $S$  on the velocity, temperature and concentration profiles for Cu-water nanofluid with  $P = 0.2, R = 1, M = 10^{-12}, \phi = 0.1, Sc = \lambda = 1$

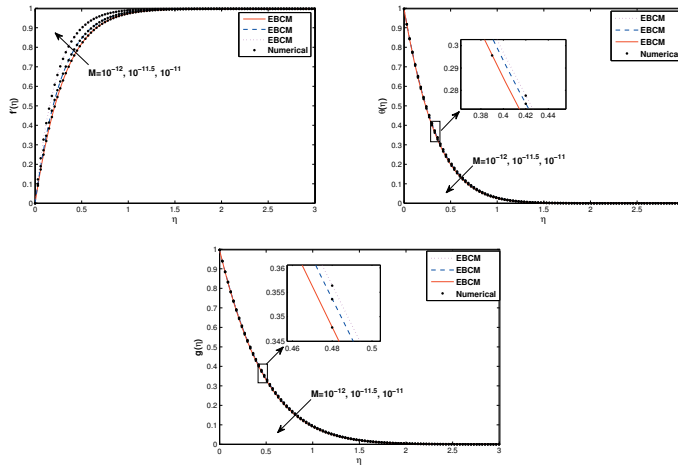


**Figure 7.** Effect of the magnetic parameter  $M$  on the velocity, temperature and concentration profiles for Cu-water nanofluid with  $P = 0.5, R = S = 1, \phi = 0.1, Sc = \lambda = 1$

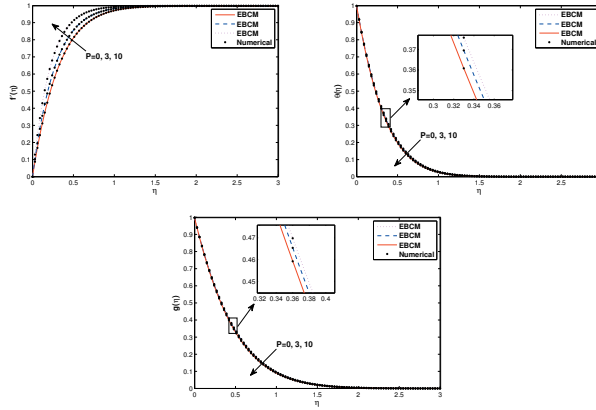


**Figure 8.** Effect of the permeability parameter  $P$  on the velocity, temperature and concentration profiles for Cu-water nanofluid with  $M = 10^{-12}$ ,  $R = S = 1$ ,  $\phi = 0.1$ ,  $Sc = \lambda = 1$ .

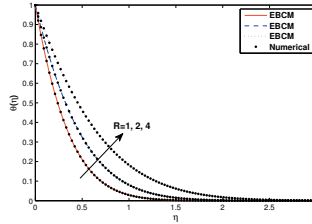


**Figure 9.** Effect of the radiation parameter  $R$  on the temperature profiles for Cu-water nanofluid with  $M = 10^{-12}$ ,  $S = 1$ ,  $P = 0.5$ ,  $\phi = 0.1$ ,  $Sc = \lambda = 1$ .

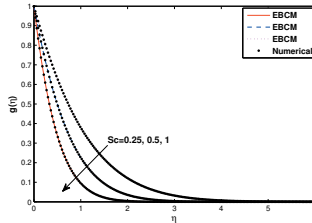


**Figure 10.** Effect of the Schmidt number  $Sc$  on the concentration profiles for Cu-water nanofluid with  $M = 10^{-12}$ ,  $P = S = \lambda = R = 1$ ,  $\phi = 0.1$ .

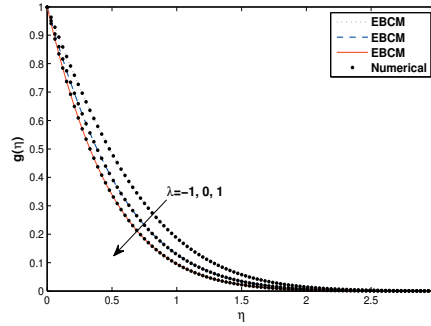


**Figure 11.** Concentration profiles for different values of the chemical reaction coefficient  $\lambda$  for Cu-water nanofluid with  $M = 10^{-12}, P = S = Sc = R = 1, \phi = 0.1$ .

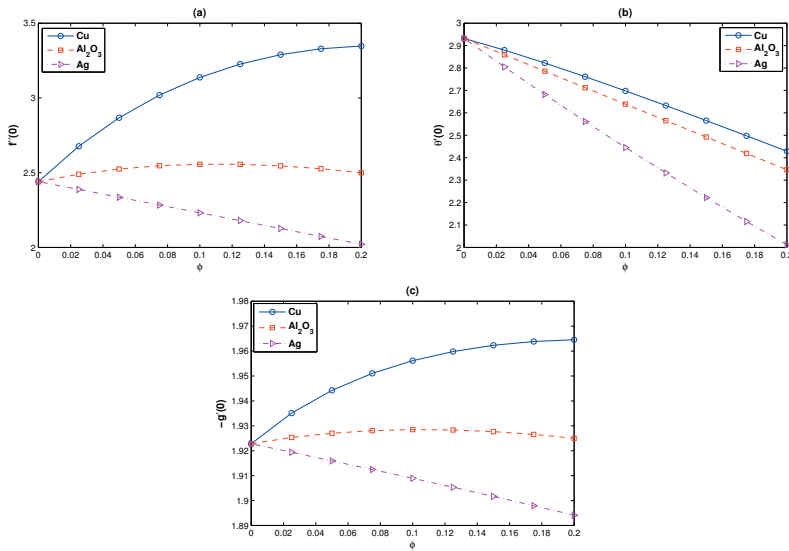


**Figure 12.** Local skin friction ( $f''(0)$ ), Local Nusselt number ( $-\theta'(0)$ ), Local Sherwood number ( $-g'(0)$ ) for different nanofluids with  $M = 10^{-12}, Sc = R = S = 1, P = 0.5$

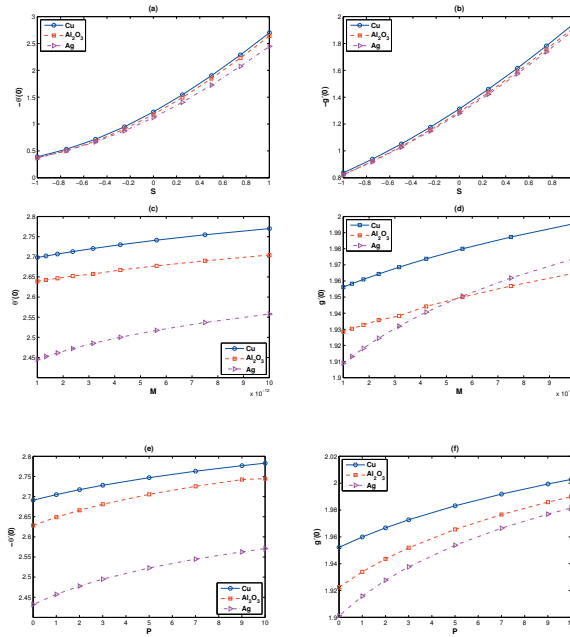


**Figure 13.** Local Nusselt number( $-\theta'(0)$ ) and Local Sherwood number( $-g'(0)$ ) for the different nanofluids; (a), (b) with  $M = 10^{-12}, Sc = \lambda = R = 1, P = 0.5, \phi = 0.1$ ; (c), (d) with  $Sc = \lambda = R = S = 1, P = 0.5, \phi = 0.1$  and (e), (f) with  $M = 10^{-12}, Sc = \lambda = R = S = 1, \phi = 0.1$ .

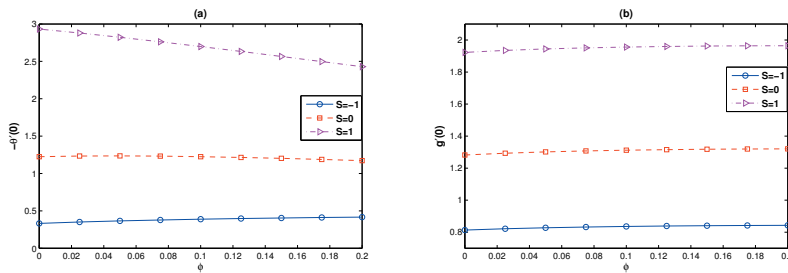


**Figure 14.** Local Nusselt number( $-\theta'(0)$ ) and Local Sherwood number( $-g'(0)$ ) for different value nanoparticle volume friction and the suction/blowing parameter for Cu-water nanofluid with  $M = 10^{-12}, Sc = \lambda = R = 1, P = 0.5$ .

**Table 2:** The value of  $-\theta'(0)$  for different values of  $\phi$ ,  $R$  when  $P = 0.5$ ,  $M = 10^{-12}$ ,  $Pr = 6.2$ 

| Cu-water                       | $\phi$ | $R$ | EBCM method | Numerical  | DTM-BF [57] |
|--------------------------------|--------|-----|-------------|------------|-------------|
|                                | 0      | 1   | 2.93179710  | 2.93178297 | 2.9174      |
|                                |        | 2   | 2.04184021  | 2.04184021 | 2.0294      |
|                                |        | 4   | 1.38340295  | 1.38340295 | 1.3733      |
|                                | 0.1    | 1   | 2.69804743  | 2.69804743 | 2.6876      |
|                                |        | 2   | 1.96056847  | 1.96056847 | 1.9518      |
|                                |        | 4   | 1.36644320  | 1.36644320 | 1.3597      |
|                                | 0.2    | 1   | 2.42892277  | 2.42892277 | 2.4201      |
|                                |        | 2   | 1.83500213  | 1.83500213 | 1.8277      |
|                                |        | 4   | 1.31549420  | 1.31549419 | 1.3101      |
| Al <sub>2</sub> O <sub>3</sub> | $\phi$ | $R$ | EBCM method | Numerical  | DTM-BF [57] |
|                                | 0      | 1   | 2.93178297  | 2.93178297 | 2.9174      |
|                                |        | 2   | 2.04184021  | 2.04184021 | 2.0294      |
|                                |        | 4   | 1.38340295  | 1.38340295 | 1.3733      |
|                                | 0.1    | 1   | 2.63895590  | 2.63895590 | 2.6269      |
|                                |        | 2   | 1.91088707  | 1.91088707 | 1.9007      |
|                                |        | 4   | 1.32919074  | 1.32919073 | 1.3211      |
|                                | 0.2    | 1   | 2.34650710  | 2.34650710 | 2.3358      |
|                                |        | 2   | 1.76416100  | 1.76416100 | 1.7551      |
|                                |        | 4   | 1.26121445  | 1.26121445 | 1.2542      |
| Ag-water                       | $\phi$ | $R$ | EBCM method | Numerical  | DTM-BF [57] |
|                                | 0      | 1   | 2.93178297  | 2.93178297 | 2.9174      |
|                                |        | 2   | 2.04184021  | 2.04184021 | 2.0294      |
|                                |        | 4   | 1.38340295  | 1.38340295 | 1.3733      |
|                                | 0.1    | 1   | 2.44536904  | 2.44536904 | 2.4348      |
|                                |        | 2   | 1.77740432  | 1.77740432 | 1.7688      |
|                                |        | 4   | 1.24151765  | 1.24151765 | 1.2351      |
|                                | 0.2    | 1   | 2.01155861  | 2.01155861 | 2.0037      |
|                                |        | 2   | 1.52515709  | 1.52515709 | 1.5191      |
|                                |        | 4   | 1.10041408  | 1.10041409 | 1.0966      |

**Table 3:** The value of  $-g'(0)$  for different values of  $\phi, Sc$  when  $P = 0.5, M = 10^{-12}, \lambda = 1$

| Cu-water                       | $\phi$ | $Sc$ | EBCM method | Numerical  | DTM-BF [57] |
|--------------------------------|--------|------|-------------|------------|-------------|
|                                | 0      | 0.25 | 0.84744828  | 0.84744970 | 0.8438      |
|                                |        | 0.5  | 1.25732922  | 1.25732921 | 1.2530      |
|                                |        | 1    | 1.92281238  | 1.92281238 | 1.9172      |
|                                | 0.1    | 0.25 | 0.86185861  | 0.86185857 | 0.8428      |
|                                |        | 0.5  | 1.27997745  | 1.27997745 | 1.2776      |
|                                |        | 1    | 1.95614475  | 1.95614475 | 1.9525      |
|                                | 0.2    | 0.25 | 0.86531695  | 0.86531691 | 0.8525      |
|                                |        | 0.5  | 1.28554259  | 1.28554259 | 1.2838      |
|                                |        | 1    | 1.96454941  | 1.96454941 | 1.9616      |
| Al <sub>2</sub> O <sub>3</sub> | $\phi$ | $Sc$ | EBCM method | Numerical  | DTM-BF [57] |
|                                | 0      | 0.25 | 0.84744974  | 0.84744970 | 0.8438      |
|                                |        | 0.5  | 1.25732922  | 1.25732921 | 1.2530      |
|                                |        | 1    | 1.92281238  | 1.92281238 | 1.9172      |
|                                | 0.1    | 0.25 | 0.84990964  | 0.84990960 | 0.8472      |
|                                |        | 0.5  | 1.26118727  | 1.26118727 | 1.2580      |
|                                |        | 1    | 1.92848139  | 1.92848139 | 1.9241      |
|                                | 0.2    | 0.25 | 0.84829471  | 0.84829467 | 0.8464      |
|                                |        | 0.5  | 1.25872893  | 1.25872893 | 1.2561      |
|                                |        | 1    | 1.92499188  | 1.92499188 | 1.9211      |
| Ag-water                       | $\phi$ | $Sc$ | EBCM method | Numerical  | DTM-BF [57] |
|                                | 0      | 0.25 | 0.84744974  | 0.84744970 | 0.8438      |
|                                |        | 0.5  | 1.25732922  | 1.25732921 | 1.2530      |
|                                |        | 1    | 1.92281238  | 1.92281238 | 1.9172      |
|                                | 0.1    | 0.25 | 0.84018109  | 0.84083841 | 0.8397      |
|                                |        | 0.5  | 1.24740659  | 1.24740659 | 1.2453      |
|                                |        | 1    | 1.90893530  | 1.90893530 | 1.9055      |
|                                | 0.2    | 0.25 | 0.83357955  | 0.83357950 | 0.8340      |
|                                |        | 0.5  | 1.23668395  | 1.23668395 | 1.2359      |
|                                |        | 1    | 1.89415921  | 1.89415921 | 1.8920      |

## References

- [1] A. Alsaedi, M. Awais, and T. Hayat, Effects of heat generation/absorption on stagnation point flow of nanofluid over a surface with convective boundary conditions, *Commun. Nonlinear Sci. Numer. Simulion.*, 17 (2012), 4210-4223.
- [2] S. M. Aminossadati and B. Ghasemi, Natural convection cooling of a localized heat source at the bottom of a nanofluid-filled enclosure, *Eur. J. Mech. B Fluids*, 28 (2009), 630-640.
- [3] M. I. Anwar, I. Khan, S. Sharidan, and M. Z. Salleh, Magneto hydrodynamic and radiation effects on stagnation point flow of nanofluid towards a nonlinear stretching sheet, *Indian J. Chem. Technol.*, 21 (2014), 199-204.
- [4] N. Bachok, A. Ishak, and I. Pop, Boundary layer stagnation-point flow and heat transfer over an exponentially stretching/shrinking sheet in a nanofluid, *Int. J. Heat Mass Transf.*, 55 (2012), 8122-8128.
- [5] M. A. Bellucci, On the explicit representation of shifted orthonormal Bernstein polynomials, *arXiv preprint arXiv:1404.2293*, (2014).
- [6] D. D. Bhatta and M. I. Bhatti, Numerical solution of KdV equation using modified Bernstein polynomials, *Appl. Math. Comput.*, 174 (2006), 1255-1268.
- [7] K. Bhattacharyya, Steady boundary layer flow and reactive mass transfer past an exponentially stretching surface in an exponentially moving free stream, *J. Egypt. Math. Soc.*, 20 (2012), 223-228.
- [8] K. Bhattacharyya, Boundary layer flow and heat transfer over an exponentially shrinking sheet, *Chin. Phys. Lett.*, 28 (2011), 701-704.
- [9] S. Bhattacharya and B. N. Mandal, Use of Bernstein polynomials in numerical solutions of Volterra integral equations, *Appl. Math. Sci.*, 2 (2008), 1773-1787.
- [10] M. I. Bhatti and P. Bracken, Solutions of differential equations in a Bernstein polynomial basis, *Com. Appl. Math.*, 205 (2007), 272-280.
- [11] J. P. Boyd, The optimization of convergence for Chebyshev polynomial methods in an unbounded domain, *J. Comput. Phys.*, 45 (1982), 43-79.
- [12] J. P. Boyd, Chebyshev and Fourier spectral methods, *2nd edn. Dover Publications Inc., Mineola*, (2001).

- [13] J. Buongiorno, Convective transport in nanofluids, *ASME J. Heat Transf.*, 128 (2006), 240-250.
- [14] A. Chakrabarti and S. C. Martha, Approximate solutions of Fredholm integral equations of the second kind, *Appl. Math. Comput.*, 211 (2009), 459-466.
- [15] T. C. Chiam, Stagnation-point flow towards a stretching plate, *J. Phys. Soc. Jpn.*, 63 (1994), 2443-2444.
- [16] S. U. S. Choi and J. A. Eastman, Enhancing thermal conductivity of fluids with nanoparticles, *ASME International Mechanical Engineering Congress and Exposition, San Francisco*, (1995), 99-105.
- [17] E. H. Doha, A. H. Bhrawy, and M. A. Saker, On the derivatives of Bernstein polynomials: An application for the solution of high even-order differential equations, *Boundary Value Problems*, (2011).  
doi:10.1155/2011/829543.
- [18] E. H. Doha, A. H. Bhrawy, and M. A. Saker, Integrals of Bernstein polynomials: An application for the solution of high even-order differential equations, *Appl. Math. Lett.*, 24 (2011), 559-565.
- [19] G. Farin, *Curves and Surfaces for Computer Aided Geometric Design*, Academic Press, Boston, Mass, USA, (1996).
- [20] R. T. Farouki and T. N. T. Goodman, On the optimal stability of Bernstein basis, *Math. Comp.*, 65 (1996), 1553-1566.
- [21] F. Garoosi, L. Jahanshaloo, M. M. Rashidi, A. Badakhsh, and M. A. Ali, Numerical Simulation of Natural Convection of the Nanofluid in Heat Exchangers using a Buongiorno Model, *Appl. Math. Comput.*, 254 (2015), 183-203.
- [22] S. D. Harris, D. B. Ingham, and I. Pop, Mixed convection boundary layer flow near the stagnation point on a vertical surface in a porous medium: Brinkman model with slip, *Transp. Porous Media*, 77 (2009), 267-285.
- [23] M. Heydari, G. B. Loghmani, and S. M. Hosseini, Exponential Bernstein functions: An effective tool for the solution of heat transfer of a micropolar fluid through a porous medium with radiation, *Comput. Appl. Math.*, 36 (2017), 647-675.

- [24] M. Heydari, G. B. Loghmani, M. M. Rashidi, and S. M. Hosseini, A numerical study for off-centered stagnation flow towards a rotating disc, *Propulsion and Power Research.*, 4 (2015), 169-178.
- [25] K. Hiemenz, Die grenzschicht an einem in den gleichformigen flussigkeitsstrom eingetauchten geraden kreiszylinder, *Dingle's Polytech. J.*, 326 (1911), 321-340.
- [26] E. Hosseini, G. B. Loghmani, M. Heydari, and M. M. Rashidi, Investigation of magneto-hemodynamic flow in a semi-porous channel using orthonormal Bernstein polynomials, *Eur. Phys. J. Plus.*, (2017), 321-326.
- [27] E. Hosseini, G. B. Loghmani, M. Heydari, and M. M. Rashidi, Numerical investigation of velocity slip and temperature jump effects on unsteady flow over a stretching permeable surface, *Eur. Phys. J. Plus.*, (2017), 96-132.
- [28] E. Hosseini, G. B. Loghmani, M. Heydari, and A. M. Wazwaz, A numerical study of electrohydrodynamic flow analysis in a circular cylindrical conduit using orthonormal Bernstein polynomials, *Computational Methods for Differential Equations*, 5 (2017), 280-300.
- [29] W. Ibrahim and O. D. Makinde, The effect of double stratification on boundary-layer flow and heat transfer of nanofluid over a vertical plate, *Comput. Fluids*, 86 (2013), 433-441.
- [30] A. Ishak, MHD boundary layer flow due to an exponentially stretching sheet with radiation effect, *Sains Malays.*, 40 (2011), 391-395.
- [31] D. D. Joseph, D. A. Nield, and G. Papanicolaou, Nonlinear equation governing flow in a saturated porous media, *Water Resour. Res.*, 18 (1982), 1049-1052.
- [32] P. K. Kameswaran, M. Narayana, P. Sibanda, and P. V. S. N. Murthy, Hydromagnetic nanofluid flow due to a stretching or shrinking sheet with viscous dissipation and chemical reaction effects, *Int. J. Heat Mass Transf.*, 55 (2012), 7587-7595.
- [33] P. P. Korovkin, Interpolation and approximation by polynomials: Bernstein polynomials, *Springer encyclopedia of mathematics*, (2001).
- [34] E. Kreyszig, *Introductory Functional Analysis with Applications*, Wiley, New York, (1978).

- [35] A. V. Kuznetsov and D. A. Nield, Natural convection boundary-layer of a nanofluid past a vertical plate: a revised model, *Int. J. Therm. Sci.*, 77 (2014), 126-129.
- [36] O. D. Makinde, Analysis of Sakiadis flow of nanofluids with viscous dissipation and Newtonian heating, *Appl. Math. Mech.*, 12 (2012), 1545-1554.
- [37] O.D. Makinde, Computational modelling of nanofluids flow over a convectively heated unsteady stretching sheet, *Curr. Nanosci.*, 9 (2013), 673-678.
- [38] O. D. Makinde, Effects of viscous dissipation and Newtonian heating on boundary layer flow of nanofluids over a flat plate, *Int. J. Numer. Methods Heat Fluid Flow*, 23 (2013), 1291-1303.
- [39] O. D. Makinde and A. Aziz, Boundary layer flow of a nanofluid past a stretching sheet with a convective boundary condition, *Int. J. Therm. Sci.*, 50 (2011), 1326-1332.
- [40] K. Maleknejad, E. Hashemizadeh, and B. Basirat, Computational method based on Bernstein operational matrices for nonlinear Volterra-Fredholm-Hammerstein integral equations, *Commun. Nonlinear. Sci. Numer. Simulat.*, 17 (2012), 52-61.
- [41] K. Maleknejad, E. Hashemizadeh, and R. Ezzati, A new approach to the numerical solution of Volterra integral equations by using Bernstein's approximation, *Commun. Nonlinear. Sci. Numer. Simulat.*, 16 (2011), 647-655.
- [42] B. N. Mandal and S. Bhattacharya, Numerical solution of some classes of integral equations using Bernstein polynomials, *Appl. Math. Comput.*, 190 (2007), 1707-1716.
- [43] I. C. Mandal and S. Mukhopadhyay, Heat transfer analysis for fluid flow over an exponentially stretching porous sheet with surface heat flux in porous medium, *Ain Shams Eng. J.*, 4 (2013), 103-110.
- [44] W. N. Mutuku-Njane and O. D. Makinde, Combined effect of buoyancy force and Navier slip on MHD flow of a nanofluid over a convectively heated vertical porous plate, *Sci. World J.*, <http://dx.doi.org/10.1155/2013/725643>.
- [45] W. N. Mutuku-Njane and O. D. Makinde, MHD nanofluid flow over a permeable vertical plate with convective heating, *J. Comput. Theor. Nanosci.*, 11 (2014), 667-675.

- [46] H. Masuda, A. Ebata, K. Teramae, and N. Hishinuma, Alteration of thermal conductivity and viscosity of liquid by dispersing ultra-fine particles, *Netsu Bussei*, 7 (1993), 227-233.
- [47] D. A. Nield and A. Bejan, *Convection in Porous Media*, Springer, New York, (2006).
- [48] H. F. Oztop and E. Abu-Nada, Numerical study of natural convection in partially heated rectangular enclosures with nanofluids, *Int. J. Heat Fluid Flow*, 29 (2008), 1326-1336.
- [49] D. Pal and P. S. Hiremath, Computational modeling of heat transfer over an unsteady stretching surface embedded in a porous medium, *Meccanica*, 45 (2010), 415-424.
- [50] D. Pal and G. Mandal, Influence of thermal radiation on mixed convection heat and mass transfer stagnation-point flow in nanofluids over stretching/shrinking sheet in a porous medium with chemical reaction, *Nucl. Eng. Des.*, 273 (2014), 644-652.
- [51] S. Rosseland, *Theoretical Astrophysics*, Oxford Universit, New York, (1936).
- [52] D. Rostamy and K. Karimi, Bernstein polynomials for solving fractional heat- and wave-like equations, *Fract. Calc. Appl. Anal.*, 15 (2012), 556-571.
- [53] C. Y. Wang, Impinging stagnation flows, *Phys. Fluids*, 30 (1987), 915-917.
- [54] S. A. Yousefi and M. Behroozifar, Operational matrices of Bernstein polynomials and their applications, *Int. J. Syst. Sci.*, 41 (2010), 709-716.
- [55] S. A. Yousefi, M. Behroozifar, and M. Dehghan, The operational matrices of Bernstein polynomials for solving the parabolic equation subject to specification of the mass, *J. Comput. Appl. Math.*, 235 (2011), 5272-5283.
- [56] S. A. Yousefi, M. Behroozifar, and M. Dehghan, Numerical solution of the nonlinear age-structured population models by using the operational matrices of Bernstein polynomials, *Appl. Math. Model.*, 36 (2012), 945-963.
- [57] C. Zhang, L. Zheng, X. Zhang, and G. Chen, MHD flow and radiation heat transfer of nanofluids in porous media with variable surface heat flux and chemical reaction, *Appl. Math. Model.*, 39 (2015), 165-181.

**Ehsan Hosseini**

Ph.D Student in the Mathematics  
Department of Mathematics  
Yazd University  
Yazd, Iran  
E-mail: ehsanhoseini66@gmail.co

**Ghasem Barid Loghmani**

Professor of Applied Mathematics  
Department of Mathematics  
Yazd University  
Yazd, Iran  
E-mail: loghmani@yazd.ac.ir

**Mohammad Heydari**

Assistant Professor of Mathematics  
Department of Mathematics  
Yazd University  
Yazd, Iran  
E-mail: m.heydari@yazd.ac.ir

**Mohammad Mehdi Rashidi**

Professor of Mechanical Engineering  
Department of Civil Engineering  
School of Engineering  
University of Birmingham  
Birmingham, UK  
E-mail: m.m.rashidi@bham.ac.uk